NANOSYSTEMS

SYNTHESIS OF NANO-SIZED $TiO_2/ZrO_2/SiO_2$ DISPERSIONS AND STUDY OF THEIR STRUCTURAL, OPTICAL, AND PHOTOCATALYTIC PROPERTIES

N.V. VITYUK,[1] G.M. EREMENKO,[1] N.P. SMIRNOVA,[1] T.O. BUSKO,[2] M.P. KULISH,[2] O.P. DMYTRENKO,[2] V.O. GOLUB[3]

[1]**O.O. Chuiko Institute of Surface Chemistry, Nat. Acad. of Sci. of Ukraine**
(17, General Naumov Str., Kyiv 03164, Ukraine; e-mail: nvityuk@gmail.com)

[2]**Taras Shevchenko National University of Kyiv**
(64, Volodymyrs'ka Str., Kyiv 01601, Ukraine)

[3]**Institute of Magnetism, Nat. Acad. of Sci. of Ukraine**
(36-b, Vernadsky Blvd., Kyiv 03142, Ukraine)

The sol-gel method was applied to synthesize $TiO_2/ZrO_2/SiO_2$ powders (a content of 21:9:70 mol.%) with the use of various silicon dioxide sources. Using the X-ray fluorescence analysis (XFA), we found that two phases (the anatase and srilankite ones) are crystallized simultaneously in all synthesized composites. The electron paramagnetic resonance (EPR) method was used to study the paramagnetic centers, which are formed on the anatase surface, and the influence of high-energy radiation on a change of the defect structure in corresponding specimens. A relationship between the defect structure of ternary composites and their photocatalytic activity has been established.

1. Introduction

Materials fabricated on the basis of SiO_2 and doped with TiO_2 and/or ZrO_2 possess physical properties, which are improved in comparison with those of one-component oxides. In particular, these are an ultralow temperature expansion, a high refractive index, and others [1, 2]. In the optical industry [3], such materials are synthesized as anti-reflecting thin-film coatings with a required value of refractive index. The properties of such materials strongly depend on the method of their synthesis, their chemical composition, homogeneity, and crystal structure. The sol-gel method, which is widely applied to synthesize nano-sized oxide materials, consists in hydrolyzing the precursor of metal alkoxide and the following condensation. This method allows one to reach a high degree of flexibility while creating mixed oxides, because their properties can be purposely changed by varying the parameters of their synthesis procedure. The homogeneity of a composition is monitored by controlling the type of alkoxides, the solution temperature, and the precursor concentration. At the same time, the degree of hydrolysis strongly affects both the degree of surface hydroxylation and various structural aspects. The processes of solution aging, drying, and subsequent thermal treatment allow an additional control over the material structure to be executed [4].

The combination of titanium dioxide with silicon and zirconium dioxides is known to make it possible to increase the specific surface of synthesized specimens, obtain anatase particles with small dimensions, and elevate the temperature of the phase transition of anatase in rutile [3].

Preliminarily, we have synthesized binary TiO_2/ZrO_2 films with various contents of zirconium dioxide. We found that specimens with a dioxide zirconium content of 30% were the most active photocatalytically in the course of reduction of six-valent chromium ions [5]. In a number of processes aimed at the photocatalytic purification, photodestruction of organic contaminations in large volumes of aqueous solutions, adsorption/catalytic destruction, and so forth, it is more expedient to use dispersed materials on the basis of titanium dioxide and its composites, by using no substrates, which are usually applied to fix film materials of the same composition. In

this work, just such a ratio between titanium and zirconium dioxides with the addition of 70% of silicon dioxide was used. The role of SiO_2 in such composites consists in increasing the specific surface of specimens, enhancing their thermal stability, and improving the uniformity of the active-phase nanoparticle distribution over the surface. This work aimed at synthesizing $TiO_2/ZrO_2/SiO_2$ (21:9:70 mol.%) photocatalysts, which are active in redox processes, making use of different SiO_2 sources, in order to study the influence of SiO_2 on structural, optical, and photocatalytic properties of composites, as well as on their stability with respect to high-energy radiation.

2. Experimental Part

In this work, we synthesized $TiO_2/ZrO_2/SiO_2$ powders taking advantage of titanium and zirconium tetraisopropoxides as sources of Ti and Zr, respectively, and a number of SiO_2 sources, namely, tetraethoxysilane (TEOS); a stable colloid of SiO_2 Ludox, a 30 % suspension in water, with the specific surface $S_{sp} = 220$ m^2/g and pH = 8.9, Aldrich; and Davisil silica gel, $S_{sp} = 480$ m^2/g, 99 % Aldrich. Initial solutions were obtained by carrying out common hydrolysis of $Ti(OPr)_4$, $Zr(OPr)_4$, and $Si(OC_2H_5)_4$/Ludox/Davisil, by using acetylacetone (AcAc) as a complexing agent to slow down the hydrolysis rate of Ti and Zr alkoxides. After the jellification of the solutions, the corresponding powders were obtained. All the specimens were calcined at $T = 600$ °C, with the heating rate amounting to 0.3 °C/ min.

The specific surface of $TiO_2/ZrO_2/SiO_2$ powders was determined on a Kelvin-1042 installation (Costech International Instruments) following the argon adsorption technique (the Brunauer–Emmett–Teller (BET) method).

The crystalline structure of $TiO_2/ZrO_2/SiO_2$ powders was determined using X-ray diffractometry. Diffraction patterns of $TiO_2/ZrO_2/SiO_2$ specimens were registered on a Dron-4-07 diffractometer using the radiation of CuK$_\alpha$-line emitted by the anode with a nickel filter. The measurements were carried out in the reflected beam and the Bragg–Brentano registration geometry.

The structure of paramagnetic centers in the obtained specimens was studied using the EPR method. For this purpose, we used a Bruker Elexis E-500 radio spectrometer operating in the X-range at a constant frequency of 9.867152 GHz and at room temperature. Before the registration of spectra, the specimens

were blown through with argon. The g-factors were calculated using the formula $h\nu = g\beta H$, where H is the magnetic field strength, ν the frequency, h Planck's constant, and β the atomic magnetism unit (the Bohr magneton). The relative determination error for g was ± 0.001. The magnitudes of g-factor in the EPR spectra were determined following the method reported in work [6].

High-energy irradiation of the specimen was carried, by using an ILU-6 electron accelerator. The electron energy was 1.9 MeV, the electron beam current $I = 4$ mA, and the exposure dose varied from 0.5 to 4.0 Gy.

The diffusion reflection spectra of ternary $TiO_2/ZrO_2/SiO_2$ powders were registered with the help of a Lambda Bio 35 Perkin–Elmer spectrophotometer with a Labsphere RSA-PR-20 integrating sphere in a wavelength range of 200–1000 nm. The "Spectralon" was used as a standard reference specimen. Absorption spectra were obtained from the corresponding reflection spectra using the Kubelka–Munk formula.

The photocatalytic activity of nano-sized $TiO_2/ZrO_2/SiO_2$ composites was examined by carrying out photoreduction reactions of dichromate ions in the presence of the electron donor, Na$_2$EDTA, following the procedure reported in work [7]. This mixture can also be used as a model for waste water purification, where both the oxidizer and the reducer often present simultaneously.

At the photoreduction of dichromate ions, the initial concentration of $K_2Cr_2O_7$ in the aqueous solution and Na$_2$EDTA was 4×10^{-4} mol/l. The solutions were irradiated in a temperature-stabilized quartz reactor 40 ml in volume. The temperature of the reaction medium was 22 ± 1 °C. Irradiation was carried out in the presence of a photocatalyst 4 ± 1 g in mass. At the irradiation, the reaction mixture was stirred in air by a magnetic mixer. As a source of UV light, we used a DRT-1000 high-pressure mercury lamp. The absorption spectra of solutions were studied before and after the irradiation with the help of a Lambda UV-Vis spectrophotometer (Perkin Elmer) in a quartz cuvette 1 cm in thickness. The content of dichromate ions was monitored by observing the variation of the optical density of a solution at a wavelength of 350 nm, which corresponded to Cr(VI) ions in the course of irradiation. The reaction rates were calculated using the kinetic equation of the pseudo first order and with the relative error ± 0.1. The pH of a solution was controlled by adding $HClO_4$ and monitored using an I-129.1 ionometer.
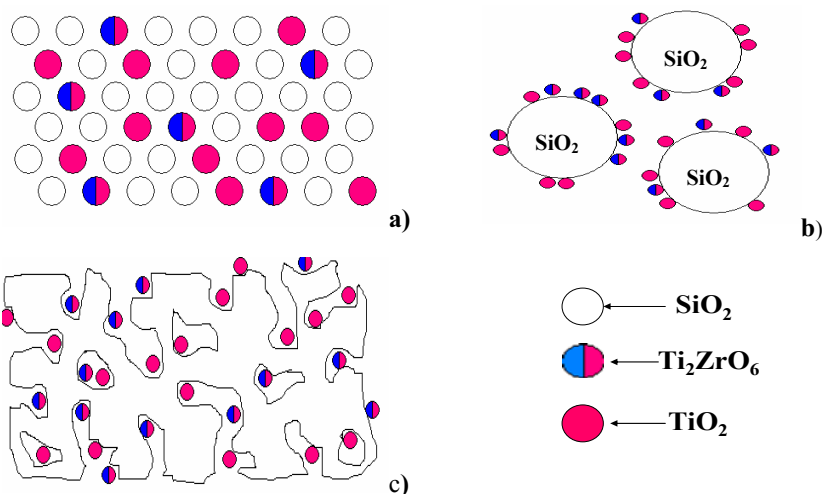
Fig. 1. Schematic diagrams for the distributions of components in $TiO_2/ZrO_2/SiO_2$ powders fabricated using different sources of silicon dioxide: (*a*) tetraethoxysilane (TEOS), (*b*) colloid SiO_2 Ludox, 30%, and (*c*) Davisil silica gel
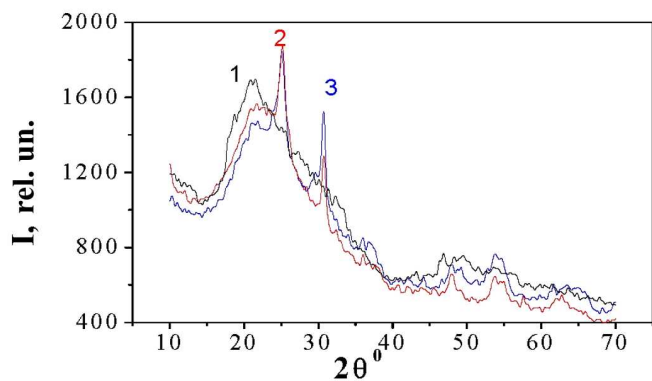

Fig. 2. Diffraction patterns of $TiO_2/ZrO_2/SiO_2$ powders synthesized using different SiO_2 sources – (*1*) TEOS, (*2*) Ludox, and (*3*) Davisil – after their temperature treatment at a temperature of 600 °C

3. Results and Their Discussion

In Fig. 1, the distributions of components in SiO_2 matrices obtained with the use of different sources of silicon dioxide are schematically shown. If all the three alkoxides were deposited simultaneously (Fig. 1,*a*), the components were uniformly distributed, and they formed a considerable quantity of common bonds. If the 30% colloid of SiO_2 Ludox was used, in which silicon dioxide particles had already been formed and were characterized by a certain size (of about 30 nm), hydrolysis of alkoxides and deposition of titanium and zirconium oxides occurred on SiO_2 particles (Fig. 1,*b*). When using Davisil, the impregnation of the alkoxide mixture into pores and onto the surface of silica gel took place.

Using the method of X-ray phase analysis, we established that two phases crystallize simultaneously in $TiO_2/ZrO_2/SiO_2$ powders fabricated by the sol-gel method. These are titanium dioxide in the anatase phase and a solid solution of titanium zirconate in the srilankite phase (Ti_2ZrO_6) [8, 9].

Figure 2 makes it evident that, in $TiO_2/ZrO_2/SiO_2$ powders obtained using TEOS, the crystallization process only starts at a treatment temperature of 600 °C. The XFA spectra for two other specimens – obtained using the stable 30% colloid of SiO_2 Ludox as a sources of SiO_2 (curve *2* in Fig. 2) or the Davisil silica gel (curve *3* in Fig. 2) – already demonstrate main peaks corresponding to the formation of two phases, anatase and srilankite.

At the further calcination of $TiO_2/ZrO_2/SiO_2$ (TEOS) powder to temperatures of 700 (curve *2* in Fig. 3) and 800 °C (curve *3* in Fig. 3), the crystallinity of a specimen and the size of crystals grow (curves *2* and *3* in Fig. 3). This fact is also verified by the appearance of main peaks, which correspond to the formation of titanium dioxide in the anatase phase (a) and titanium zirconate in the srilankite phase (s).

While studying the Raman scattering in $TiO_2/ZrO_2/SiO_2$ powders, we revealed vibrations, which, in accordance with the results of work [10], correspond to anatase (see Fig. 4). From this figure, one can see that, for $TiO_2/ZrO_2/SiO_2$ (TEOS) powders, crystallization begins at higher temperatures, which is in agreement with the XFA data. Figure 4 also demonstrates that, depending on the SiO_2 source used for synthesizing $TiO_2/ZrO_2/SiO_2$ powders, a shift
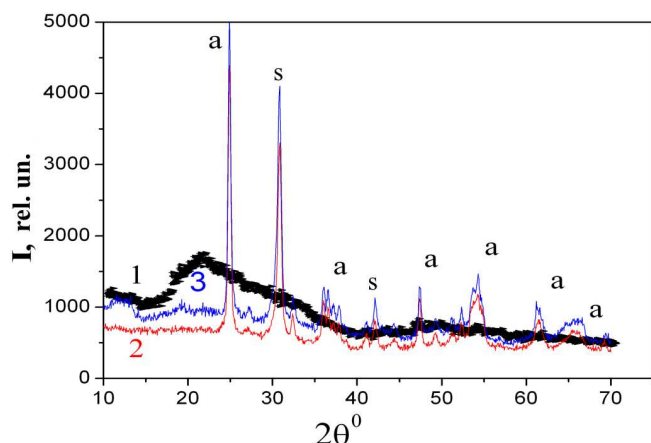
Fig. 3. Diffraction pattern of TiO$_2$/ZrO$_2$/SiO$_2$ (TEOS) powder fabricated using the sol-gel method after the precursor jellification and calcined at various temperatures of (*1*) 600, (*2*) 700, and (*3*) 800 °C
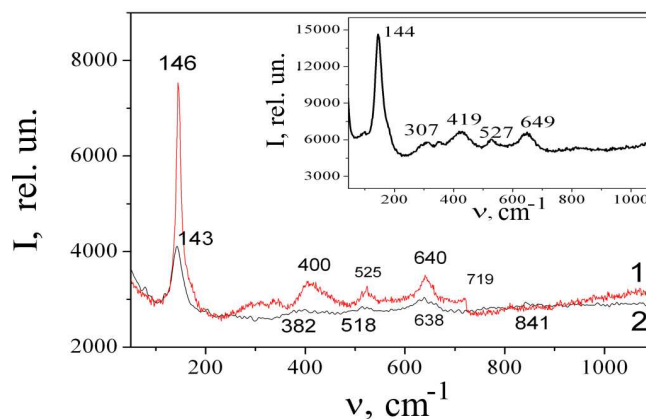

Fig. 4. Raman shift spectra of powders after their heat treatment at a temperature of 600 °C: (*1*) TiO$_2$/ZrO$_2$/SiO$_2$ (Davisil) and (*2*) TiO$_2$/ZrO$_2$/SiO$_2$ (Ludox). The same, but for the TiO$_2$/ZrO$_2$/SiO$_2$ (TEOS) powder after its heat treatment at a temperature of 800 °C, is depicted in the inset
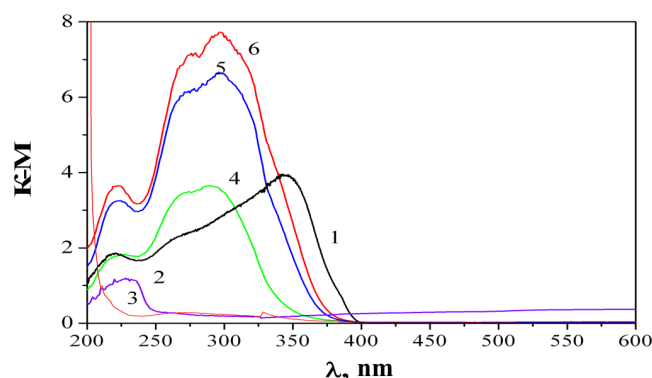
of vibration modes toward larger values takes place, which, in accordance with the results of work [10], evidences the increase of crystal dimensions. Hence, if Ludox or Davisil are used as SiO$_2$ sources, alkoxides do not mix at the molecular level. Their hydrolysis may probably run on the surface of formed silica particles. Crystallization of titanium and zirconium oxides starts at lower temperatures, so that the corresponding sizes of formed particles are larger than in the case where TEOS was used.

The absorption spectra of the one-component powders of titanium, zirconium, and silicon dioxides, as well as the mixed TiO$_2$/ZrO$_2$/SiO$_2$ oxides (Fig. 5), were obtained from the diffuse reflection spectra by using the Kubelka–Munk formula [11],

$$F(R_\infty) = (1 - R_\infty)^2/2R_\infty = \alpha/S,$$

where R_∞ is the coefficient of diffuse reflection from an infinitely thick powder layer (of an order of 2–3 mm), α is the absorption coefficient (in terms of cm^{-1} units), and S is the scattering factor; the latter is almost independent of the wavelength for particles larger than the light wavelength.

Absorption in the UV spectral range corresponds to the ligand–metal charge transfer from O^{2-} to Ti^{4+}, when an electron from the valence band (2p-O) is ex-

Fig. 5. Absorption spectra of powders after their heat treatment at a temperature of 600 °C: (*1*) TiO$_2$, (2) ZrO$_2$, (*3*) SiO$_2$, (*4*) TiO$_2$/ZrO$_2$/SiO$_2$ (TEOS), (*5*) TiO$_2$/ZrO$_2$/SiO$_2$ (Ludox), and (*6*) TiO$_2$/ZrO$_2$/SiO$_2$ (Davisil). In every ternary system, the component content is 21%:9%:70%, respectively

cited and transferred into the conduction band (3d-Ti) [12]. The mixed oxides have the absorption band maximum at energies somewhat higher in comparison with that for TiO$_2$. This may mean that the charge transfer O$^{2-} \rightarrow$ Zr^{4+} is either imposed onto or combined with the electron transfer O$^{2-} \rightarrow$ Ti^{4+} [12].

Making use of absorption spectra (Fig. 5) and knowing the absorption band edge value, we calculated the energy gap width for one- and three-component powders; the results of calculations are exhibited in Table 1. One can see that the energy values for TiO$_2$/ZrO$_2$/SiO$_2$ mixtures lie between the corresponding values for one-component titanium and zirconium oxides, which may testify to the formation of common bonds between the components.
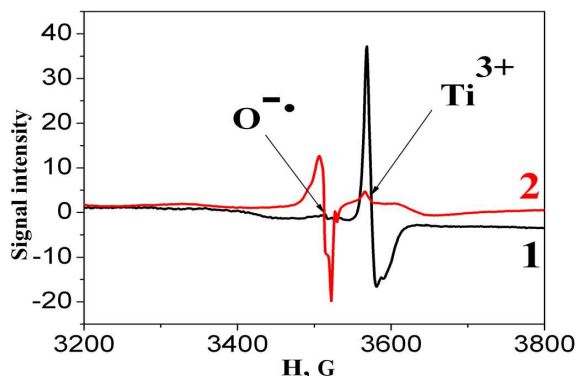
T a b l e 1. **Energy gap widths for powders**

Specimens	E_{g}, eV	Specimens	E_{g}, eV
TiO$_2$	3.3	TiO$_2$/ZrO$_2$/SiO$_2$ (TEOS)	3.7
ZrO$_2$	5.1	TiO$_2$/ZrO$_2$/SiO$_2$ (Ludox)	3.6
SiO$_2$	>6	TiO$_2$/ZrO$_2$/SiO$_2$ (Davisil)	3.5

Fig. 6. EPR spectra of $TiO_2/ZrO_2/SiO_2$ (TEOS) powder before (1) and after (2) high-energy radiation
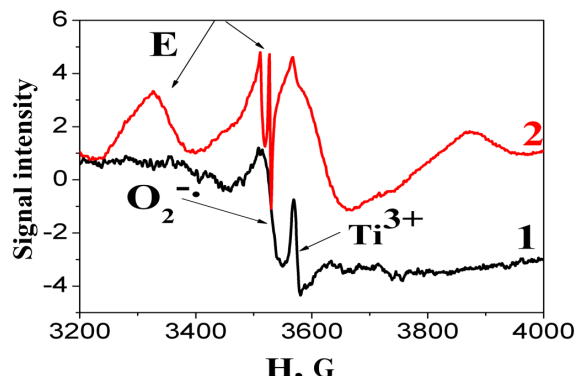

Fig. 7. EPR spectra of $TiO_2/ZrO_2/SiO_2$ (Ludox) powder before (1) and after (2) high-energy radiation

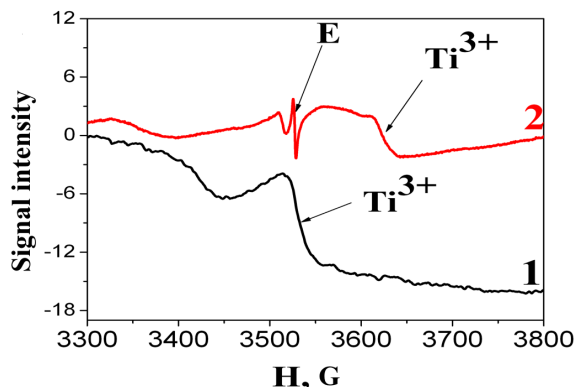Fig. 8. EPR spectra of $TiO_2/ZrO_2/SiO$ (Davisil) powder before (1) and after (2) high-energy radiation

It is known from the literature [13] that ionizing radiation stimulates the generation of such structural defects as coordinationally unsaturated Ti atoms, oxygen vacancies, OH radicals, and others, which are of importance for the catalytic action of TiO_2-based photocatalysts. To obtain the clear understanding of how the thermal treatment and high-energy radiation affect the generation of surface defects, we made a research of the defect structure using the EPR method. To study paramagnetic centers (PCs) in $TiO_2/ZrO_2/SiO_2$ powders and to elucidate how high-energy irradiation influences them, it is important to analyze the formation of PCs and their changes under the radiation action in one-component oxides [14].

From the EPR spectra obtained for a ternary system (spectrum 1 in Fig. 6), we see that, after the thermal treatment, only a signal with the axial symmetry typical of Ti^{3+} centers with g-factors $g_\perp = 1.971$ and $g_\parallel = 1.963$, which are created on titanium dioxide in the anatase phase, is formed [15–23].

After the high-energy irradiation, the character of the EPR signal changed a little. First, the intensity of the signal that corresponds to Ti^{3+} centers decreased, which testified that defects of this type became reduced at the high-energy irradiation. Second, after the irradiation (spectrum 2 in Fig. 6), other defects were formed in the range of lower fields. These were oxygen vacancies, which, in accordance with the results of works [15–23], were generated on the anatase (TiO_2) surface.

For the ternary system $TiO_2/ZrO_2/SiO_2$ synthesized with the use of the colloid SiO_2 solution–Ludox, as well as for the $TiO_2/ZrO_2/SiO_2$ (TEOS) system, an anisotropic signal with the g-factors $g_\perp = 1.996$ and $g_\parallel = 1.958$ was observed in the high-field interval after the thermal treatment at a temperature of 600 °C had been applied (spectrum 1 in Fig. 7). According to the results of work [24], this signal can be associated with the formation of Ti^{3+} centers on the anatase surface.
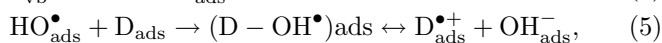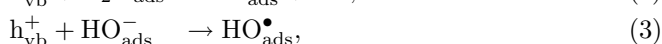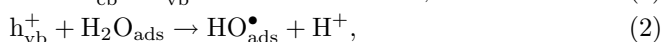
A new signal typical of irradiated SiO_2 [14] appeared in the EPR spectra after the high-energy irradiation (spectrum 2 in Fig. 7). It means the formation of defects–namely, oxygen vacancies–both on the surface and in the bulk of silicon dioxide [25–31]. The signal corresponding to the formation of Ti^{3+} the centers was also available, but it was shifted to the higher-field interval, with the corresponding g-factors being $g_\perp = 1.945$ and $g_\parallel = 1.923$.

For a powder of the $TiO_2/ZrO_2/SiO_2$ ternary system synthesized with the use of Davisil silica gel, two signals were observed after the thermal treatment(spectrum 1 in Fig. 8). The first signal was anisotropic. It was observed at higher fields and, as in the previous cases, corresponded to the formation of Ti^{3+} centers with the corresponding g-factors $g_\perp = 1.972$ and $g_\parallel = 1.959$ on the titanium dioxide surface. The other signal was observed in the range of lower fields. It corresponded to the

formation of oxygen vacancies on the titanium dioxide surface.

After this system had been subjected to high-energy irradiation, a new signal, similarly to the previous case, was formed. In accordance with the results of work [27], it can be associated with the formation of defects in the bulk, P_b, and on the surface, E', of SiO$_2$. The signal in the higher-field region, which can be connected with vacancies of the Ti^{3+} type, disappeared from the EPR spectrum. This resulted in a reduction of the photocatalytic activity of the corresponding powders.

The universal mechanism governing the formation of two types of charge carriers in the bulk of semiconductors at their irradiation with light with the quantum energy $E > E_g$ allowed us to propose them as effective photocatalysts in the processes of water purification from harmful organic substances and heavy-metal ions. The well-known mechanism of charge generation for a photocatalytic process to run is described by the following sequence of equations [32]:

$$SC \rightarrow e_{cb}^- + h_{vb}^+ \quad \rightarrow \text{recombination}, \tag{1}$$

$$h_{vb}^+ + H_2O_{ads} \rightarrow HO_{ads}^\bullet + H^+, \tag{2}$$

$$h_{vb}^+ + HO_{ads}^- \quad \rightarrow HO_{ads}^\bullet, \tag{3}$$

$$h_{vb}^+ + D_{ads} \rightarrow D_{ads}^{\bullet+}, \tag{4}$$

$$HO_{ads}^\bullet + D_{ads} \rightarrow (D - OH^\bullet)ads \leftrightarrow D_{ads}^{\bullet+} + OH_{ads}^-, \tag{5}$$

$$e_{cb}^- + A_{ads} \rightarrow A_{ads}^{\bullet-}, \tag{6}$$

where SC stands for a semiconductor; D and A are a donor and an acceptor, respectively; and h$^+$ and e$^-$ are a photogenerated hole and an electron, respectively.

In the course of the photoreduction of potassium dichromate in the presence of our ternary system prepared using TEOS, Ludox, and Davisil calcined at a temperature of 600 °C (Fig. 9), the complete restoration of six-valent chromium ions to three-valent ones was observed. The kinetic curves of the potassium dichromate photoreduction allowed us to calculate the corresponding rate constants. The obtained values are quoted in Table 2, where the calculated values for the specific surface in the powders of TiO$_2$/ZrO$_2$/SiO$_2$ system are exhibited as well.

T a b l e 2. **Dependence of rate constants for the photoreduction of potassium dichromate on the specific surface of specimen**

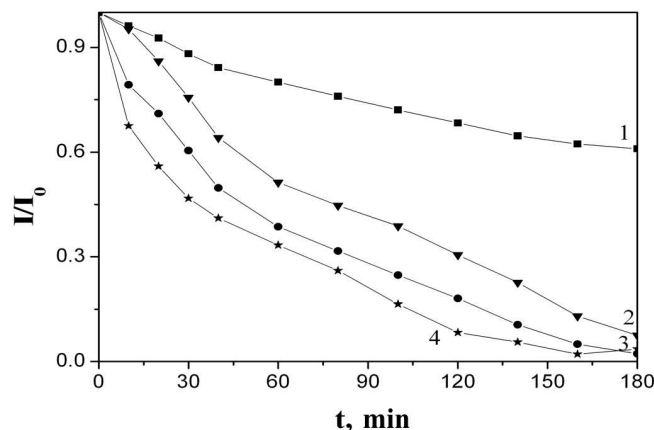|	Specimen	S_{sp}, m^2/g	Rate constant κ, min^{-1}
1.	TiO$_2$/ZrO$_2$/SiO$_2$ (TEOS)	< 4	1.2×10^{-2}
2.	TiO$_2$/ZrO$_2$/SiO$_2$ (Ludox)	165	1.8×10^{-2}
3.	TiO$_2$/ZrO$_2$/Si$_2$ (Davisil)	190	2.6×10^{-2}

Fig. 9. Curves of potassium dichromate photorestoration kinetics in the presence of EDTA on the powders of ternary system after their heat treatment at a temperature of 600 °C: (1) reference specimen, (2) TiO$_2$/ZrO$_2$/SiO$_2$ (TEOS), (3) TiO$_2$/ZrO$_2$/SiO$_2$ (Ludox), and (4) TiO$_2$/ZrO$_2$/SiO$_2$ (Davisil). The ratio I/I_0 corresponds to the changes of the absorption maximum intensity of dichromate ions as a function of the UV-irradiation time

Figure 9 and Table 2 demonstrate that the catalyst synthesized using Davisil silica gel (scheme 1) is characterized by the largest specific surface and more effective photocatalytic properties. We also see that the specific surfaces of TiO$_2$/ZrO$_2$/SiO$_2$ (Ludox) and TiO$_2$/ZrO$_2$/SiO$_2$ (Davisil) specimens exceed very much the specific surface of TiO$_2$/ZrO$_2$/SiO$_2$ (TEOS) specimen. However, despite such a large difference between the specific surface values (190, 165, and 4 m^2/g, respectively), the activity of the obtained photocatalysts in the photoreduction of Cr(VI) ions do not differ from one another so substantially. This means that the influence of the specific surface on the photocatalytic activity is not so strong as that of defects, which are formed in the synthesized specimens. As was marked above, while synthesizing powders with the use of tetraethoxysilane in the course of the common hydrolysis, a uniform distribution of components over the photocatalyst surface takes place, and the formation of paramagnetic centers (Ti^{3+}) on the surface attains its maximum. It is the presence of those centers in the course of thermal treatment that results in a considerable photocatalytic activity of the corresponding specimens.

Under the action of high-energy irradiation, defects of various types are formed on the surface of TiO$_2$/ZrO$_2$/SiO$_2$ powders synthesized using different SiO$_2$ sources. For TiO$_2$/ZrO$_2$/SiO$_2$ (Ludox) and TiO$_2$/ZrO$_2$/SiO$_2$ (Davisil) specimens, these are defects in the bulk (P$_b$-centers), which are deep traps for elec-
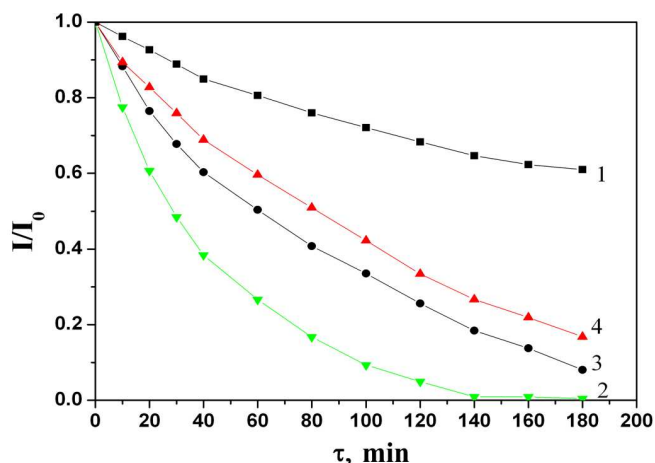
Fig. 10. Kinetic curves for the photoreduction of potassium dichromate in the presence of EDTA on powders of the ternary system after the heat treatment at a temperature of 600 °C and high-energy irradiation: (1) reference specimen, (2) $TiO_2/ZrO_2/SiO_2$ (TEOS), (3) $TiO_2/ZrO_2/SiO_2$ (Ludox), and (4) $TiO_2/ZrO_2/SiO_2$ (Davisil)

trons. Therefore, the photocatalytic activity of those specimens will decrease.

In Fig. 10, the kinetic curves obtained for the process of Cr(VI) ion reduction in the presence of photocatalysts $TiO_2/ZrO_2/SiO_2$ (TEOS), $TiO_2/ZrO_2/SiO_2$ (Ludox), and $TiO_2/ZrO_2/SiO_2$ (Davisil) after β-irradiation had been applied are depicted. The kinetic curves were used to calculate the photoreduction rate constants for $TiO_2/ZrO_2/SiO_2$ powders. The obtained values are quoted in Table 3. Figure 10 and Table 3 testify that the rate constants became half as high for $TiO_2/ZrO_2/SiO_2$ (Ludox) and $TiO_2/ZrO_2/SiO_2$ (Davisil) specimens after their high-energy irradiation. Such a decrease in the activity of photocatalysts confirms the important roles that the formation of structural defects plays, as well as the influence of defects on the charge separation processes at UV-irradiation.

The photocatalytic activity of ternary $TiO_2/ZrO_2/SiO_2$ (TEOS) powders after the high-energy irradiation grew in the course of reduction of Cr(VI) ions owing to the formation of active centers on

T a b l e 3. **Rate constants for the photoreduction of potassium dichromate in the presence of $TiO_2/ZrO_2/SiO_2$ powders after high-energy irradiation**

Specimen	Rate constant κ, min^{-1}
$TiO_2/ZrO_2/SiO_2$ (TEOS)	2.5×10^{-2}
$TiO_2/ZrO_2/SiO_2$ (Ludox)	1.1×10^{-2}
$TiO_2/ZrO_2/SiO_2$ (Davisil)	1.0×10^{-2}

the anatase surface, which promoted a deceleration of charge recombination processes.

4. Conclusions

The crystalline structure of $TiO_2/ZrO_2/SiO_2$ powders obtained by the sol-gel method has been studied. It is found that the simultaneous crystallization of two phases – titanium dioxide in the anatase phase and titanium zirconate in the srilankite phase – took place. Crystallization of $TiO_2/ZrO_2/SiO_2$ powders obtained using tetraethoxysilane as a source of SiO_2 began later than that of $TiO_2/ZrO_2/SiO_2$ (Ludox) and $TiO_2/ZrO_2/SiO_2$ (Davisil) powders, which corresponds to the data obtained with the use of the XFA and Raman spectroscopy methods.

In the course of researches of paramagnetic centers and the influences of high-energy radiation on them, we have found that the application of different SiO_2 sources gives rise to the formation of paramagnetic centers of different types. In the case of $TiO_2/ZrO_2/SiO_2$ (TEOS) powder, these are Ti^{3+} centers and oxygen vacancies on the anatase surface. In the case of $TiO_2/ZrO_2/SiO_2$ (Ludox) and $TiO_2/ZrO_2/SiO_2$ (Davisil) specimens, these are Ti^{3+} centers and oxygen vacancies on the anatase surface before irradiation, and Ti^{3+} centers on the anatase surface and oxygen vacancies on the surface (E-centers) and in the volume (P_b-centers) of silicon dioxide after irradiation.

Such differences in the formation of corresponding structural defects in ternary $TiO_2/ZrO_2/SiO_2$ systems synthesized with the use of different SiO_2 sources differently affect their photocatalytic activity. In the case of non-irradiated specimens, the highest activity was observed for $TiO_2/ZrO_2/SiO_2$ (Davisil) powders, the specific surface of which was the largest. After irradiation, the activity of $TiO_2/ZrO_2/SiO_2$ (Davisil) specimen became 2.5 times as low owing to the formation of defects on the surface and in the bulk of silicon dioxide. This occurred in contrast to $TiO_2/ZrO_2/SiO_2$ (TEOS) powders, for which their photocatalytic activity got higher, which evidences the stability of the given system to the high-energy irradiation and a possibility of its use under high-radiation conditions.

1. C.J. Brinker and A.J. Hurd, J. Phys. III (Paris) **4**, 1231 (1994).

2. M. Itoh, H. Hattori, and K. Tanabe, J. Catalys. **35**, 225 (1974).

3. P.N. Gunawidjaja, M.A. Holland, G. Mountjoy, D.M. Pickup, R.J. Newport, and M.E. Smith, Solid State Nucl. Magn. Reson. **23**, 88 (2003).

4. J.B. Miller and I. Ko, Catalys. Today **35**, 269 (1997).

5. N. Vityuk, Ya. Dyvinskyi, N. Smirnova, G. Eremenko, and O. Orans'ka, Khim. Fiz. Tekhnol. Poverkh. **9**, 76 (2003).

6. L.A. Blumenfeld, V.V. Voevodski, and A.G. Semenov, *Electron Spin Resonance in Chemistry* (Hilger, London, 1973).

7. U. Siemon, D. Bahnemann, J.J. Testa, D. Rodriguez, I. Litter, and N. Bruno, J. Photochem. Photobiol. A **148**, 247 (2002).

8. U. Diebold, Surf. Sci. Rep. **48**, 53 (2003).

9. J.-Ch. Buhl and A. Willgallis, J. Cryst. Res. Technol. **24**, 263 (1989).

10. W.F. Zhang, Y.L. He, M.S. Zhang, Z. Yin, and Q.Chen, J. Phys. D **33**, 912 (2000).

11. S. Boldish and W. White, Am. Mineralogist **83**, 865 (1998).

12. A. Dawson and P.V. Kamat, J. Phys. Chem. B **105**, 960 (2001).

13. T.O. Busko, O.P. Dmitrenko, N.P. Kulish, N.M. Belyi, N.V. Vityuk, A.M. Eremenko, N.P. Smirnova, and V.V. Shlapatsky, Vopr. At. Nauki Tekhn. N 2, 32 (2008).

14. N.V. Vityuk, G.M. Eremenko, N.P. Smirnova, and I.P. Bykov, Poverkhnya N 2, 131 (2010).

15. R. Scotti, M.D. Arienzo, A. Testino, and F. Morazzoni, Appl. Catal. B **82**, 58 (2008).

16. J.-M. Coronado, A.J. Maira, A. Martinez-Arias, J.C. Conesa, and J. Soria, J. Photochem. Photobiol. A **150**, 213 (2002).

17. C.P. Kumar, N.O. Gopal, T.C. Wang, M.-S. Wong, and S.C.Ke. J. Phys. Chem. B **110**, 5223 (2006).

18. R.F. Howe and M. Gratzel, J. Phys. Chem. **89**, 4495 (1985).

19. P. Meriaudeau, M. Che, and C.K. Jorgensen, Chem. Phys. Lett. **5**, 131 (1970).

20. J. Kiwi, J.T. Suss, and S. Szopiro, Chem. Phys. Lett. **106**, 135 (1984).

21. Y. Li, D.S. Hwang, N.H. Lee, and S.J. Kim, J. Phys. Chem. Lett. **404**, 25 (2005).

22. M. Aundaithai and T.R.N. Kutty, Mater. Res. Bull. **23**, 1675 (1988).

23. D. Zwingel, Solid State Commun. **26**, 775 (1978).

24. J. Soria, J. Sanz, I. Sobrados, J.M. Coronado, F. Fresno, and M.D. Hernandez-Alonso, Catalys. Today **129**, 240 (2007).

25. G. Buscarino and S. Agnello, J. Non-Cryst. Solids **353**, 577 (2007).

26. P.V. Sushko, S. Mukhopadhyay, A.M. Stoneham, and A.L. Shluger, Microelectr. Eng. **80**, 292 (2005).

27. S. Angello, N. Chiodini, A. Paleari, and A. Parlato, J. Non-Cryst. Solids **353**, 573 (2007).

28. D.L. Griscom, Phys. Rev. B. **20**, 1823 (1979).

29. M. Boero, A. Pasquarello, J. Sarnthein, and R. Car, Phys. Rev. Lett. **78**, 887 (1997).

30. T. Uchino, M. Takahashi, and T. Yoko, Phys. Rev. Lett. **86**, 5522 (2001).

31. V.V. Afanas'ev and A Stesmans, J. Phys.: Condens. Matter **12**, 2285 (2000).

32. H. Fu, G. Lu, and S. Li, J. Photochem. Photobiol. A **114**, 81 (1998).

СИНТЕЗ, СТРУКТУРНІ, ОПТИЧНІ
ТА ФОТОКАТАЛІТИЧНІ ВЛАСТИВОСТІ
НАНОРОЗМІРНИХ ДИСПЕРСІЙ TiO$_2$/ZrO$_2$/SiO$_2$

Н.В. Вітюк, Г.М. Єременко, Н.П. Смірнова, Т.О. Буско, М.П. Куліш, О.П. Дмитренко, В.О. Голуб

Р е з ю м е

Золь-гель методом синтезовано порошки TiO$_2$/ZrO$_2$/SiO$_2$ (21/9/70 мол.%) з використанням різних джерел діоксиду кремнію. Методом РФА встановлено, що у всіх синтезованих композитах відбувається одночасна кристалізація двох фаз (анатазу та шриланкіту). Методом ЕПР досліджено парамагнітні центри, що формуються на поверхні анатазу, і вплив високоенергетичного опромінення на зміну дефектної структури відповідних зразків. Встановлено зв'язок між дефектною структурою потрійних композитів та їх фотокаталітичною активністю.